J Nanostruct 16(2): 1733-1743, Spring 2026

RESEARCH PAPER

# Role of Micro/Nano porous Activated Carbon Prepared from Black Olive Pits Against Oleandrin-Induced Toxicity in Vital Organs of Albino Rats

***Duha Mohammed Mortatha***

*Department of Pharmaceutics and Pharmaceutical Industry, Faculty of Pharmacy, Kufa University, Iraq*

**ARTICLE INFO**

***Article History:***
*Received 22 December 2025*
*Accepted 26 March 2026*
*Published 01 April 2026*

***Keywords:***
*Adsorption*
*Intestines*
*Lung*
*Micro/Nano porous*
*stomach*

**ABSTRACT**

In order to determine the impact of the oleandrin compound on specific essential organs( lung,stomach and intestines) of white rats both before and after the adsorption process, adsorption was carried out using activated carbon made from black olive pits gathered in Iraq. The findings showed that the oleandrin clearly had a detrimental effect on the organs under investigation before therapy. Nevertheless, a noticeable improvement was seen following adsorption onto the activated carbon, indicating that the adsorption method was successful in lowering the toxicity of the chemical and enhancing its biological response. Furthermore, a thorough analysis of the adsorption process was carried out, encompassing a number of influencing factors like temperature, pH, equilibrium time, and the ideal dosage of adsorbent. In order to ascertain the adsorption mechanism and gain a better understanding of the interaction between the oleandrin being studied and the adsorbent surface, kinetic experiments were also conducted, and the adsorption was of the pseudo-second-order type and coincided with the Freundlich isotherm.

**How to cite this article**
*Mohammed Mortatha D. Role of Micro/Nano porous Activated Carbon Prepared from Black Olive Pits Against Oleandrin-Induced Toxicity in Vital Organs of Albino Rats. J Nanostruct, 2026; 16(2):1733-1743. DOI: 10.22052/JNS.2026.02.025*

## INTRODUCTION

Because Nerium oleander contains a number of chemicals that can be harmful when consumed in large amounts, particularly by animals, it has long been regarded as poisonous. Oleandrigenin and oleandrin, two cardiac glycosides with a poor therapeutic index that may be harmful if taken in excess, are among them [1]. Evaluation of cross-reactivity is necessary for every assay since digoxin immunoassays' detection of oleandrin and oleandrigenin varies between assays and between congeners. The fact that oleandrin and oleandrigenin block Na,K-ATPase indicates that they most likely work by inhibiting sodium pump action to produce their harmful effects. When oleander intake is suspected in cases of digitalis-like poisoning, a combination of digoxin immunoassays may be helpful in successfully ruling out oleander [2].

The surface phenomenon known as adsorption uses the same process to eliminate both organic and inorganic pollutants. Some of the solute molecules from the solution are concentrated or deposited at the solid surface as a result of liquid-solid intermolecular forces of attraction that bring the solid surface with a highly porous structure and a solution containing absorbable solute together [3]. The creation of an adsorbed

* *Corresponding Author Email: duham.najaf@uokufa.edu.iq*

**This work is licensed under the Creative Commons Attribution 4.0 International License.**
To view a copy of this license, visit http://creativecommons.org/licenses/by/4.0/.

phase with a configuration different from the bulk fluid phase is the foundation of separation by adsorption technology [4]. In a bulk material, other atoms meet all of the constituent atoms' bonding requirements, whether they are metallic, covalent, or ionic [5]. Because the atoms of the adsorbent are not entirely encircled by other adsorbent atoms, adsorbates may be driven to its surface [6]. Although the precise type of contact will depend on the species involved, the adsorption process is often classified as either physisorption, which is characterized by weak Van Der Waals forces, or chemisorption, which is indicative of covalent bonding [7]. A microcrystalline type of carbon with a porous structure that has developed internal porosity is called activated charcoal (AC). In addition to having a large surface area and strong surface reactivity, AC is very porous. The vast specific surface area of AC, which varies from 500 to 2000 $m^2/g$, is the main physical property that permits the physical adsorption of gases, vapors, and dissolved or dispersed chemicals from liquids [8]. The AC has a large internal surface area due to its numerous microscopic holes, or microspores, which accounts for its high adsorption capacity [9]. They are therefore effective adsorbents for

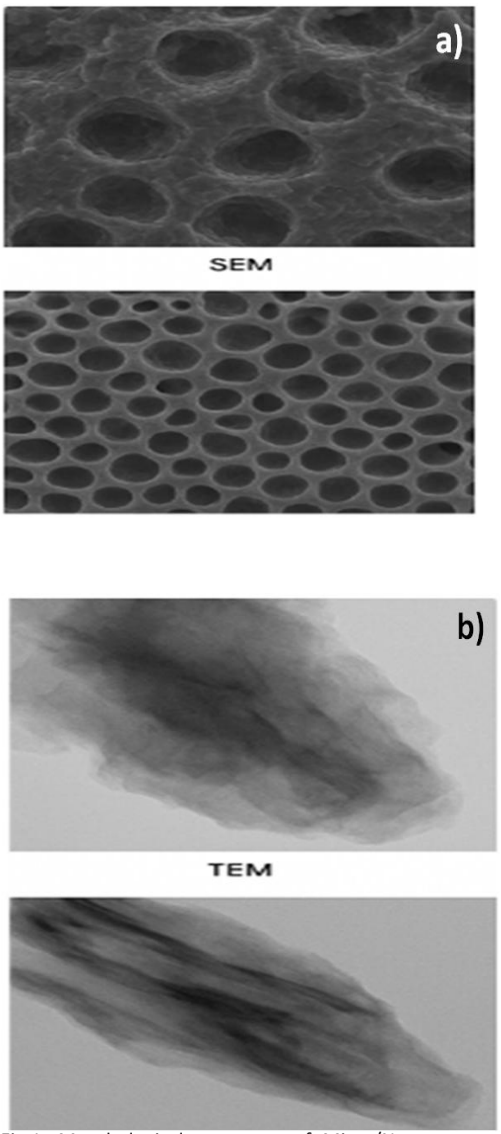


Fig.1. Morphological structures of Micro/Nano porous Activated Carbon a) FE-SEM and b) TEM image.


CC BY

a variety of troublesome chemical compounds, including inorganic, organic, microbial, and biological ones, in the treatment of water and and cases of poisoning [10].

## MATERIALS AND METHODS

Oleandrin (chemical formula: $C_{32}H_{48}O_9$; molecular weight: 576.7g $mol^{-1}$, $\lambda_{max}$ = 226nm), black olive pits, sodium hydroxide (NaOH), sodium chloride (NaCl), phosphoric acid($H_3pO_4$) and hydrochloric acid (HCl). For each analyte, 0.5 g of weight was dissolved in 2 ml of chloroform and added to 500 ml of distilled water at a concentration of 1000 ppm to make the standard stock solution of oleandrin.To be used in further research, this stock is stored in the freezer.

*Materials characterization*

The extremely porous and uneven surface morphology of the activated carbon made from black olive pits was visible in scanning electron microscopy (SEM) pictures as shown in Fig. 1a, suggesting that both micro- and mesoporous structures successfully developed during the activation process [11]. The elimination of volatile organic components during carbonization resulted in the formation of interconnecting holes and channels that gave the surface a rough appearance. The existence of nanoscale holes and partially graphitic carbon domains was further verified by Transmission Electron Microscopy (TEM) as shown in Fig. 1b, where lighter portions related to internal spaces and darker sections showed thick carbon layers [12]. The material's adsorption potential and thermal stability are both improved by this amorphous–graphitic hybrid structure.

*Preparing black olive pits charcoal (BOPC)for the adsorbent surface:*

After being collected from the Iraqi city and cleansed with water, BOPC are dried in an oven at 80°C for 48 hours. After being dried, the black olive pits are crushed into a fine powder in an oven. Powder can be activated and carbonized chemically using phosphoric acid at a 5M concentration (1:1) for 24 hours or physically using an oven at 500 °C for two hours. After being cleaned with hot water, the powder is dried and crushed to a size of 600 µm [13].

*Procedure of Adsorption*

Several flasks with 25 mL of oleandrin solution and 0.08gm of adsorbent each were filled with certain concentrations of adsorbent. The flasks are then shaken at the necessary temperature using a programmable water bath shaker at 100 rpm. After filtering the mixture, the concentration of oleandrin at equilibrium in the supernatant was measured spectrophotometrically using a UV-VIS spectrophotometer. The Eq. 1 is used to determine the adsorption capacity [14]:

$$qe = (Co\text{-}Ce) \times V/m \quad (1)$$

Where Co is the initial concentration (mg/L) and Ce (mg/L) is the concentration of the

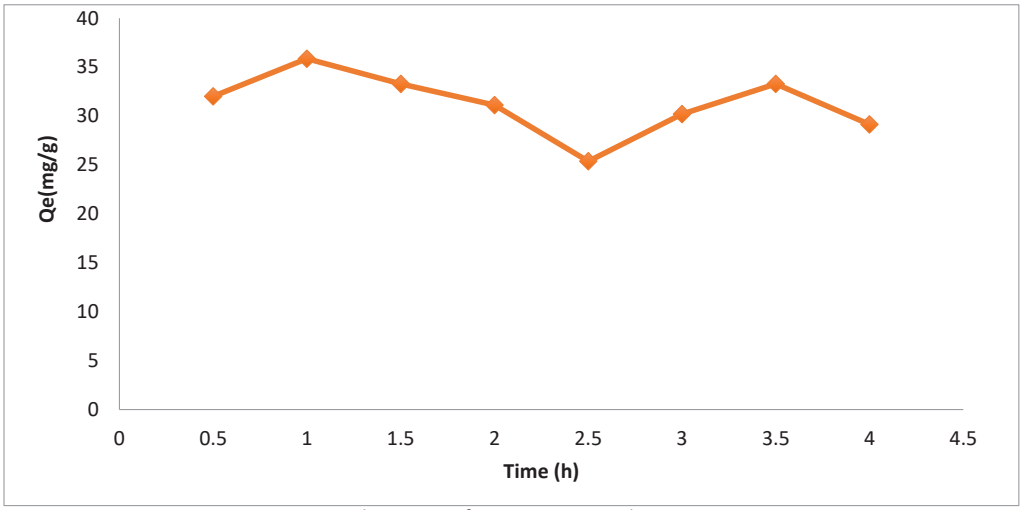


Fig.2. The impact of interaction time about BOPC.



CC BY

adsorbed oleandrin . V is the volume of solution (L) and m is the weight of adsorbent (gm).

*Animals Experiment*

In the current research, adult albino mice (Mus musculus) weighing 25–30 g were employed. The animals had free access to food and water and were kept in typical laboratory settings. The animals were divided into the following groups

Oleandrin-treated group (before adsorption): received oleandrin compound at 125ppm.

Oleandrin-treated group (after adsorption): received adsorbed oleandrin.

The laboratory animals were dissected at the conclusion of the thirty-day experiment, and a histological analysis was carried out, which included examining the histological alterations in lung,stomach and intestines.

## RESULTS AND DISCUSSION

*Contact time impact on Oleandrin elimination*

To determine the necessary adsorption time to equilibrium as a function of contact time, the adsorption of oleandrin on black olive pits was investigated. The adsorption of oleandrin by black olive pits in response to contact time is depicted in Fig. 2. Adsorption continues until equilibrium is reached, and it has been shown that the rate of adsorption first rises quickly before gradually increasing [15]. While the slow speed of oleandrin adsorption is likely as a result of solute's slow pore diffusion into most about the adsorbent, the positively charged surface of black olive pits is responsible for the quick adsorption at the first

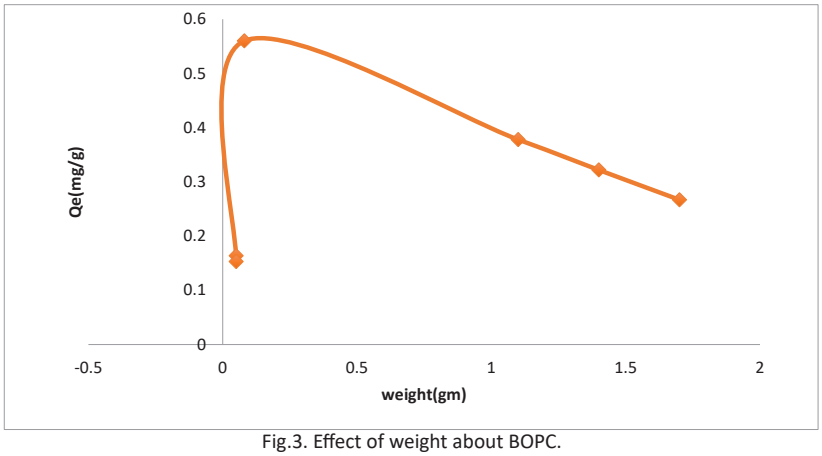


Fig.3. Effect of weight about BOPC.

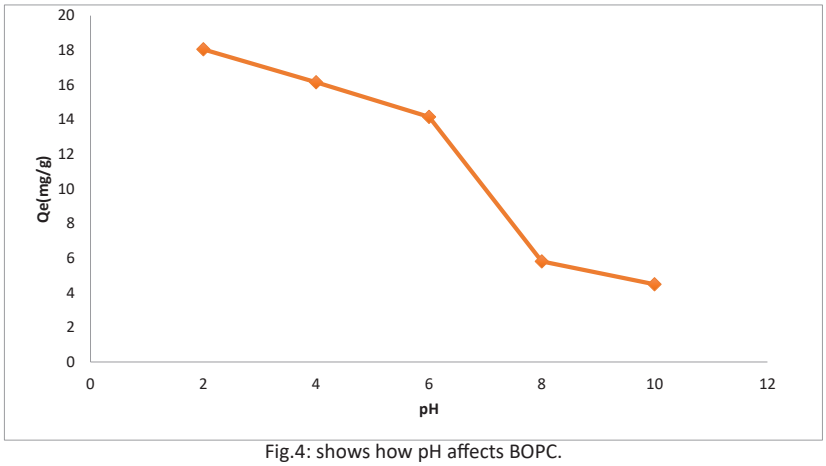


Fig.4: shows how pH affects BOPC.



CC BY

contact time [16].

*The impact of an adsorbent dosage*

The ideal weight to the reduction in the adsorption step was 0.08 gm as increasing the weight further will not improve the adsorption capacity (i.e., a steady state equilibrium will be established)..As shown in Fig. 3. This might be the result of aggregation of black olive pit charcoal at higher doses or the quick rise with in surface plus number of accessible active sites for oleandrin adsorption [17].

*Effect of pH on Oleandrin adsorption*

For BOPC, Initial pH's impact for oleandrin adsorption were examined between 2 and 10 at 298K with starting oleandrin levels equal to 275 ppm, 0.08 gm of adsorbent, and contact periods of 1 hour. Fig. 4 present the corresponding results. As may be seen, oleandrin absorption is maximum at pH 2. Because the surface is either positively charged or nearly uncharged at pH=2, oleandrin is drawn to it. [18].

*Temperature Effect*

The adsorption investigations were conducted at temperatures between 298 and 318 K. Fig. 5 highlight the process's exothermic character by showing this adsorption of oleandrin on the surface decreases with increasing temperature . It is well known that the main reason for the decreasing sorption capacity with rising

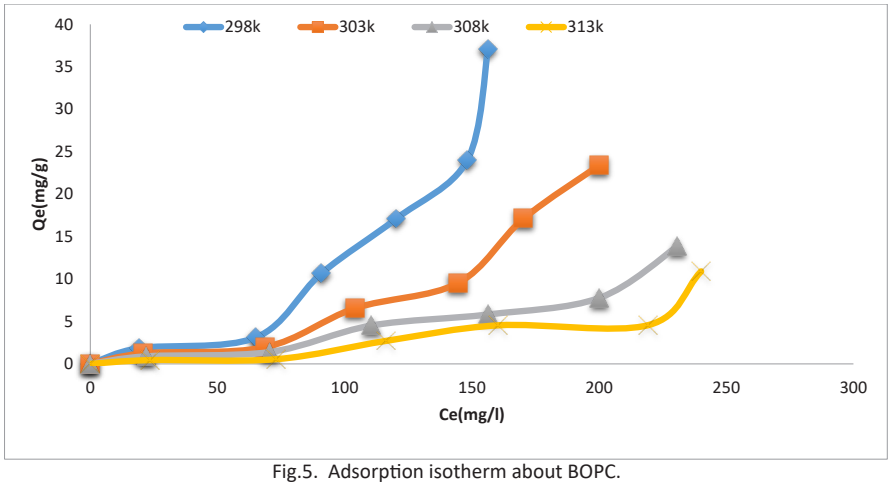


Fig.5. Adsorption isotherm about BOPC.

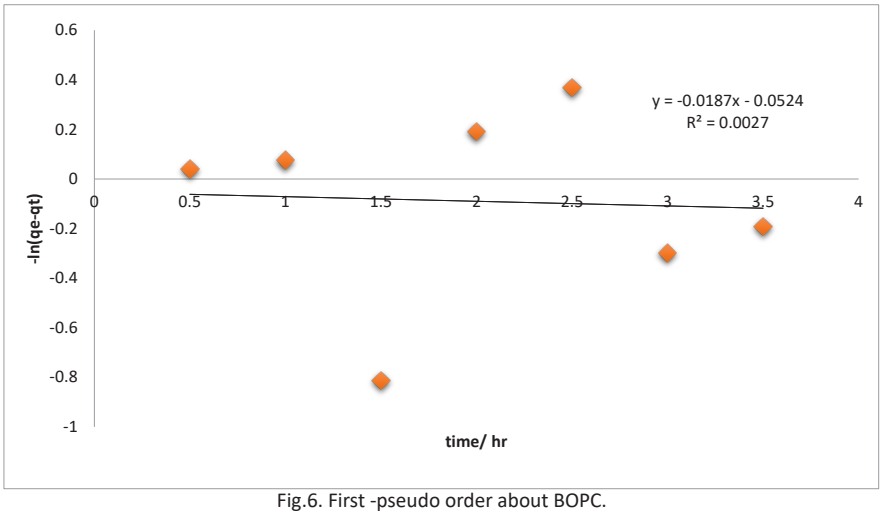


Fig.6. First -pseudo order about BOPC.

temperature is the weakening of sorption forces between the active sites on BOPC, oleandrin species, and nearby oleandrin molecules on the sorbed phase. For a typical physisorption system, an increase in temperature usually accelerates the approach to equilibrium while decreasing the adsorption capacity [19].

*Kinetics of Adsorption*

*The pseudo-first order kinetics model*

According to the model, the rate of change in adsorbate uptake at a specific reaction time is directly proportional to the variation in adsorbate concentration and removal rate over time. The Eq. 2 [20] represents the Largergren model:

$$\ln(qe\text{-}qt) = \ln qe - K1t \quad (2)$$

when the ln (qe – qt) data showed a linear correlation with t. Plotting ln (qe – qt) against t yields a linear relationship from which kt and qe can be calculated using the plot's slope and intercept.

*The Model pseudo-second-order [21]*

As shown in Fig. 7, the slope and intercept of the plot t/(qt) vs. t were used to calculate the pseudo-second-order rate constant K2.The approximate qe values are fairly similar to the experimental qe values, and all of the data under investigation had extremely high correlation coefficients.This confirms that the oleandrin adsorption on on black olive pit charcoal is described by the pseudo-second-order kinetics model and shows that the model is relevant to the entire adsorption process

*Isotherms of adsorption*

*The Langmuir isotherm*

Assuming that an oleandrin molecule occupies a site and that the adsorption process occurs at particular homogeneous sites within the adsorbent surface, the Langmuir isotherm is calculated. The adsorption process may be monolayer in nature since there is no longer any space for adsorption. For monolayer adsorption onto a totally homogenous surface with a finite number of identical sites and negligible interaction between adsorbed molecules, the Langmuir equation has the following linear form (Eq. 3) [22]:

$$Ce/qe = 1/K1\_qm + Ce/qm \quad (3)$$

where qm is the theoretical maximal adsorption capacity (mg/g) and Kl is the Langmuir adsorption

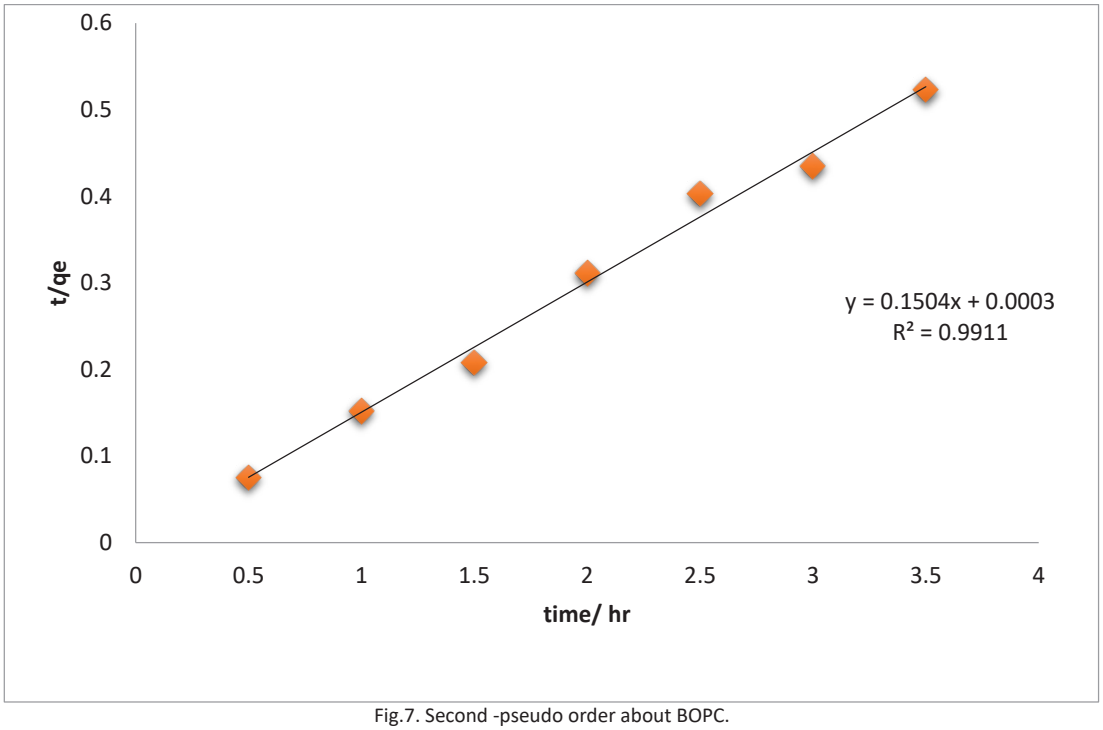


Fig.7. Second -pseudo order about BOPC.



CC BY

constant (L/mg). In Fig. 8 Ce/qe vs. Ce plots displays the correlation coefficients and the values of the Qm and Kl constants for the Langmuir isotherm.

*The isotherm Freundlich*

Is formed by reasoning this surface is heterogeneity and this heat of adsorption is spread uniformly over the surface. It was proved using the following linear form (Eq. 4) [23].

$$\log qe = \log Kf + \frac{1}{n} \log Ce \quad (4)$$

The isotherm constants Kf(L/mg) and n represent the adsorption capacity and intensity, appropriately. The 1/n factor indicates an irregular factor. Fig. 9 show the relationship between the log qe and log Ce graphs for oleandrin adsorption at 298 K.

*Biological resulst and Discussions*

In Fig. 10 show, lung tissue displayed significant pathological changes that included vascular congestion, uneven alveolar architecture, thickening of the alveolar septa, and intense

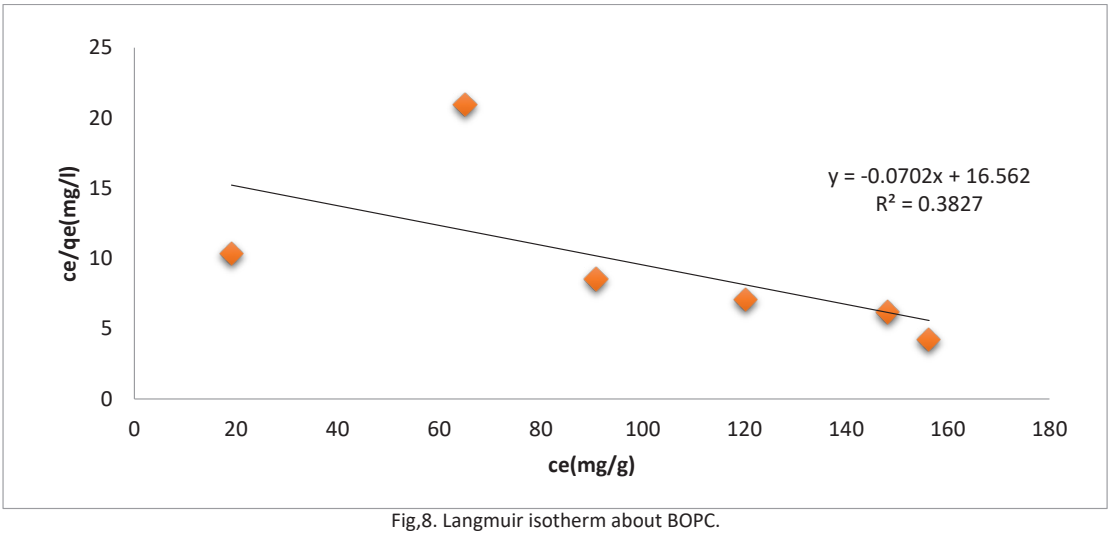


Fig,8. Langmuir isotherm about BOPC.

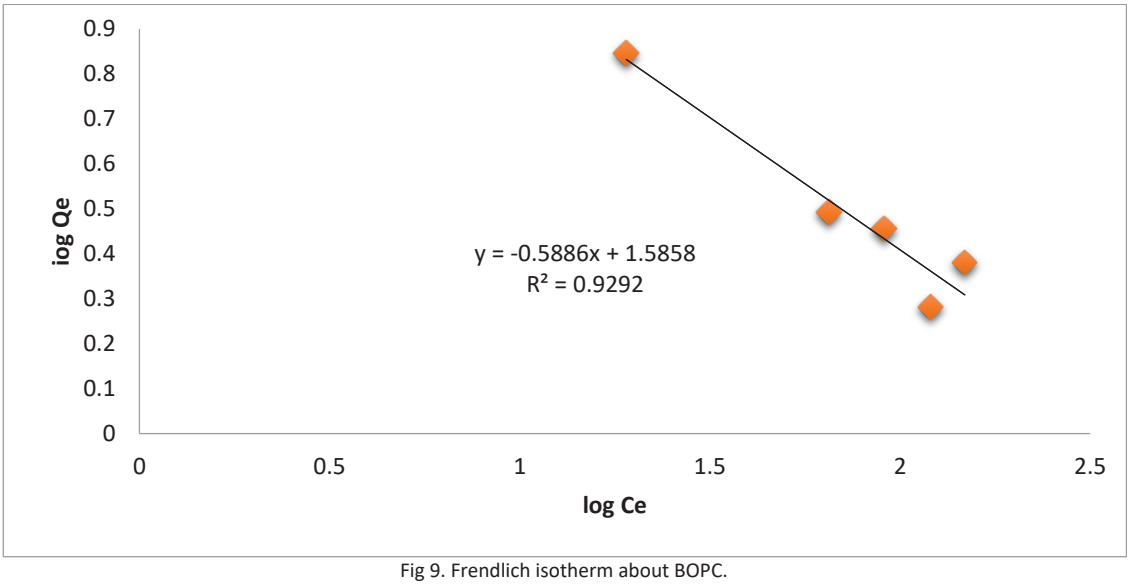


Fig 9. Frendlich isotherm about BOPC.



CC BY

infiltration of inflammatory cells inside the interalveolar spaces. These alterations reflect the toxic effect of the oleandrin and show a significant inflammatory response as well as structural damage to the pulmonary tissue [24].

On the other hand, in Fig. 11show lung tissue following adsorption showed a distinct improvement in histological architecture, with minimal inflammatory cell infiltration, mild septal thickening, and generally intact and

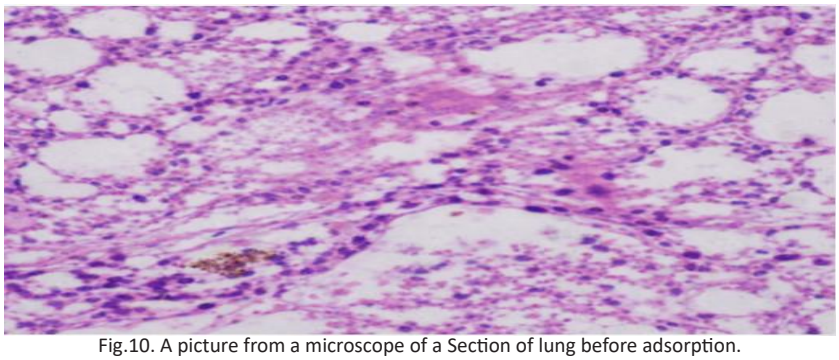

Fig.10. A picture from a microscope of a Section of lung before adsorption.

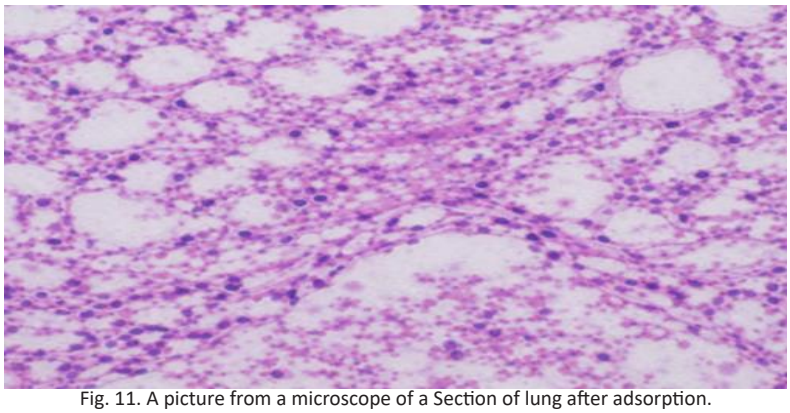

Fig. 11. A picture from a microscope of a Section of lung after adsorption.

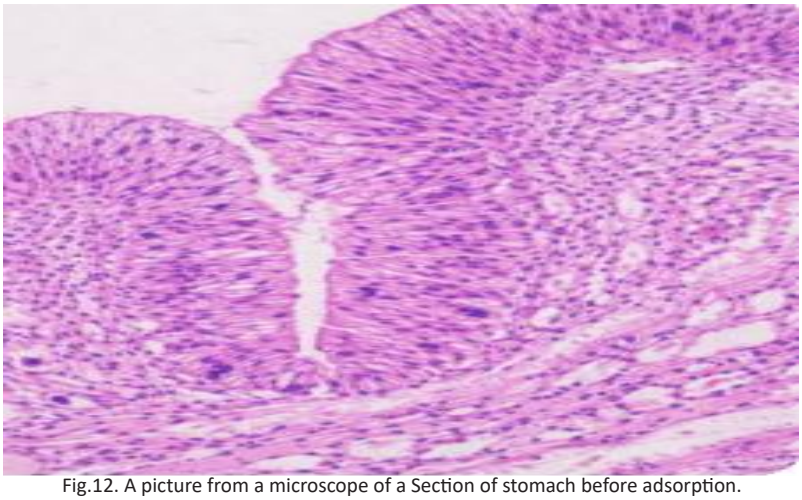

Fig.12. A picture from a microscope of a Section of stomach before adsorption.



CC BY

regularly formed alveoli. Abnormal deposits and vascular congestion were either absent or significantly decreased [25]. These results imply that by lowering the compound's bioavailability, adsorption successfully reduced its harmful effects, decreasing tissue damage and lung inflammation.

Following adsorption, in Fig. 12 stomach tissue showed significant histological changes, such as vascular congestion, intense inflammatory cell infiltration within the lamina propria, partial gastric gland degeneration, and disruption of the gastric mucosal architecture. These alterations show that the given chemical induced an immediate inflammatory response and direct toxic damage to the stomach tissue [26] In Fig. 13, stomach tissue following adsorption exhibited minor vascular congestion, comparatively undamaged gastric glands, and a significant preservation of the mucosal structure [27]. These results imply that adsorption successfully reduced the compound's harmful effects, reducing stomach tissue damage and fostering structural healing.

Significant histological changes in Fig. 14, such as severe disruption of villous architecture, villous shortening and irregularity, epithelial degeneration, and intense inflammatory cell infiltration into the lamina propria, were observed in intestinal tissue prior to adsorption. These results show direct toxic effects on the intestinal mucosa as well as acute inflammatory damage

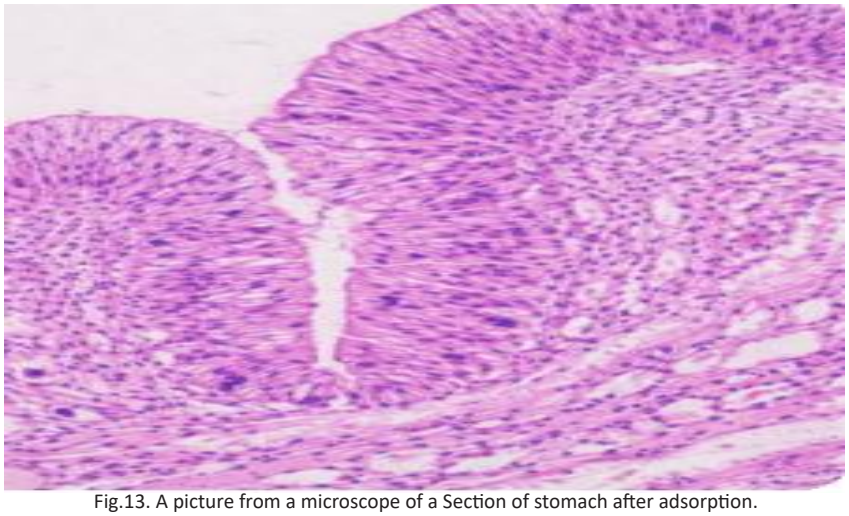

Fig.13. A picture from a microscope of a Section of stomach after adsorption.

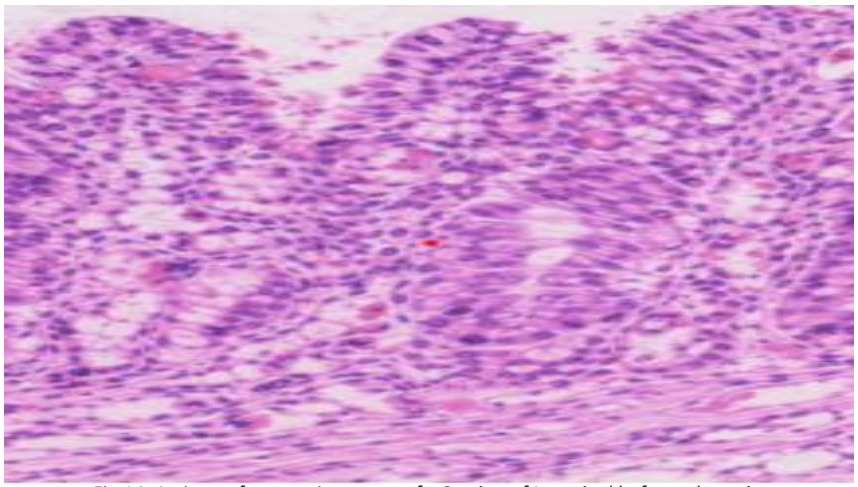

Fig.14. A picture from a microscope of a Section of Intestinal before adsorption.



CC BY

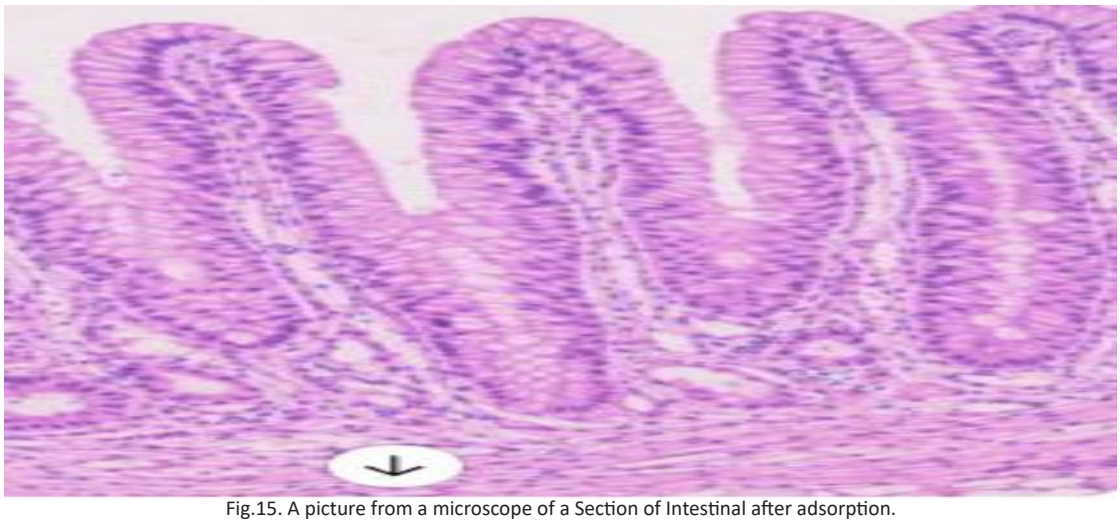

Fig.15. A picture from a microscope of a Section of Intestinal after adsorption.

[28].On the other hand, intestinal tissue following adsorption showed in Fig. 15 a significant improvement in histological structure, with intact epithelial lining, well-preserved and regularly distributed villi, and noticeably less inflammatory cell infiltration. protecting the integrity of the intestinal mucosa [29].

## CONCLUSION

The current investigation showed that oleandrin has serious toxic effects on important organs, such as the intestines, stomach, and lung of albino rats, as shown by noticeable histological changes before adsorption. Organ architecture and biological results were clearly improved by the adsorption of oleandrin onto activated carbon made from black olive pits, which led to a significant decrease in tissue damage and inflammatory reactions. Physicochemical factors like temperature, pH, salinity, equilibrium time, and adsorbent dosage had a significant impact on the adsorption process. The adsorption followed a pseudo-second-order model, according to kinetic analysis. Furthermore, multilayer adsorption on a heterogeneous adsorbent surface was indicated by the Freundlich isotherm, which offered the best fit for the experimental data. Overall, these results demonstrate that black olive pit-derived activated carbon is a sustainable and efficient adsorbent for lowering oleandrin toxicity. The potential use of this adsorption method in reducing the biological risks associated with harmful plant-derived chemicals is highlighted by the combined histopathological and adsorption investigations.

## CONFLICT OF INTEREST

The authors declare that there is no conflict of interests regarding the publication of this manuscript.

## REFERENCES

1. Tinelli A, Passantino G, Perillo A, Zizzo N. Accidental Oleandrum (Nerium Oleander L.) Ingestion: Anatomo-Pathological consequences in livestock species. Journal of the Hellenic Veterinary Medical Society. 2023;74(1):5089-5094.
2. Zhai J, Dong X, Yan F, Guo H, Yang J. Oleandrin: A Systematic Review of its Natural Sources, Structural Properties, Detection Methods, Pharmacokinetics and Toxicology. Front Pharmacol. 2022;13.
3. Reynel-Ávila HE, Aguayo-Villarreal IA, Diaz-Muñoz LL, Moreno-Pérez J, Sánchez-Ruiz FJ, Rojas-Mayorga CK, et al. A Review of the Modeling of Adsorption of Organic and Inorganic Pollutants from Water Using Artificial Neural Networks. Adsorption Science & Technology. 2022;2022.
4. Pérez-Botella E, Valencia S, Rey F. Zeolites in Adsorption Processes: State of the Art and Future Prospects. Chem Rev. 2022;122(24):17647-17695.
5. Yang L, He R, Chai J, Qi X, Xue Q, Bi X, et al. Synthesis Strategies for High Entropy Nanoparticles. Adv Mater. 2024;37(1).
6. Ock J, Meda RS, Vinchurkar T, Jadhav Y, Barati Farimani A. Adsorb-Agent: autonomous identification of stable adsorption configurations via a large language model agent. Digital Discovery. 2026;5(2):617-629.
7. Ahmed Alsharif M. Understanding Adsorption: Theories, Techniques, and Applications. Adsorption - Fundamental Mechanisms and Applications: IntechOpen; 2025.
8. Ganjoo R, Sharma S, Kumar A, Daouda MMA. Activated Carbon: Fundamentals, Classification, and Properties. Activated Carbon: The Royal Society of Chemistry; 2023. p.



CC BY

1-22.
9. Sharafinia S, Rashidi A, Ebrahimi A, Babaei B, Hadizadeh MH, Esrafili MD, et al. Enhanced VOCs adsorption with UIO-66–porous carbon nanohybrid from mesquite grain: A combined experimental and computational study. Sci Rep. 2024;14(1).
10. Abdelhamid HN. Nanocellulose-Based Materials for Water Pollutants Removal: A Review. MDPI AG; 2024.
11. Şirazi M, Aslan S. Comprehensive characterization of high surface area activated carbon prepared from olive pomace by KOH activation. Chem Eng Commun. 2021;208(10):1479-1493.
12. Zhang B, Qi Y. The Surface Properties and Characterization of Carbon Materials. Carbon Catalysis: CRC Press; 2024. p. 475-501.
13. Al-Jawaldeh H, Jamrah A, Al-Zghoul TM. Date Pits Activated Carbon as an Effective Adsorbent for Water Treatment Using $H_3PO_4$ And $H_2SO_4$ Activating Agents. Water Conservation and Management. 2025;9(2):01-05.
14. Zhang X, Ma C, Wen K, Han R. Adsorption of phosphate from aqueous solution by lanthanum modified macroporous chelating resin. Korean J Chem Eng. 2020;37(5):766-775.
15. Ghaedi M. Gold nanoparticle loaded activated carbon as novel adsorbent for the removal of Congo red. Indian Journal of Science and Technology. 2011;4(10):1208-1217.
16. Hu Q, Pang S, Wang D. In-depth Insights into Mathematical Characteristics, Selection Criteria and Common Mistakes of Adsorption Kinetic Models: A Critical Review. Separation and Purification Reviews. 2021;51(3):281-299.
17. Phatai P, Klinkaewnarong J, Yaiyen S. Adsorption of Methyl Violet Dye from Aqueous Solutions by Activated Carbon Produced from Tamarind Seeds. Advanced Materials Research. 2014;911:326-330.
18. Chemistry International CI. Adsorptive removal of Pb(II) and Cd(II) ions from aqueous solution onto modified Hiswa iron-kaolin clay: Equilibrium and thermodynamic aspects. Center for Open Science; 2021.
19. Ivbanikaro AE, Okonkwo JO, Sadiku ER, Maepa CE. Recent development in the formation and surface modification of cellulose-bead nanocomposites as adsorbents for water purification: a comprehensive review. J Polym Eng. 2023;43(8):680-714.
20. Edet UA, Ifelebuegu AO. Kinetics, Isotherms, and Thermodynamic Modeling of the Adsorption of Phosphates from Model Wastewater Using Recycled Brick Waste. Processes. 2020;8(6):665.
21. Adsorption technology and surface science. Interface Science and Technology: Elsevier; 2022. p. 39-64.
22. Esteves BM, Morales-Torres S, Madeira LM, Maldonado-Hódar FJ. Specific adsorbents for the treatment of OMW phenolic compounds by activation of bio-residues from the olive oil industry. J Environ Manage. 2022;306:114490.
23. Vigdorowitsch M, Pchelintsev A, Tsygankova L, Tanygina E. Freundlich Isotherm: An Adsorption Model Complete Framework. Applied Sciences. 2021;11(17):8078.
24. Newman RA, Sastry KJ, Arav-Boger R, Cai H, Matos R, Harrod R. Antiviral Effects of Oleandrin. J Exp Pharmacol. 2020;Volume 12:503-515.
25. Nb S. Nerium oleander toxicity: A review. International Journal of Advanced Academic Studies. 2022;4(3):23-32.
26. Khan AU. In-ovo Antiviral Effect of Nigella sativa Extract against Newcastle Disease Virus in Experimentally Infected Chicken Embryonated Eggs. Pak Vet J. 2018;38(04):434-437.
27. Maarouf T, Otmani I, Talbi A, Hamamdia Z, Bendali-Saoudi F, Abdennour C. Toxico-Pathological Assessement of Nerium Oleander Roots and Leaves on Wistar Rat. Uttar Pradesh Journal of Zoology. 2022:40-50.
28. Histopathology of Preclinical Toxicity Studies: Elsevier; 2012.
29. Haschek WM, Rousseaux CG, Wallig MA, Bolon B. Toxicologic Pathology: An Introduction. Haschek and Rousseaux's Handbook of Toxicologic Pathology: Elsevier; 2022. p. 1-12.


CC BY